Decimation Technique on Sierpinski Gasket in External Magnetic Field

Khalid Bannora[1], G. Ismail[1] and M. Abu Zeid[2]

1) Mathematics Department, Faculty of Science, Zagazig University, Zagazig, Egypt
2) Basic Science Department, Higher Technological Institute, 10th of Ramadan City, Egypt

The recursion relations of random frustrated Ising spin systems on the Sierpinski gasket placed into an external magnetic field are carried out. Spin glass (SG) and $\pm J$ model at zero and non-zero temperature are investigated. Numerical results show the effect of the external magnetic field on the flow of the probability distribution, the scaling properties of stiffness energy and the mean value of the exchange couplings. The free energy decreases exponentially with the external magnetic field. It increases algebraically as the concentration of negative bonds increases.

1. Introduction:

Fractal geometry provides a general framework for the study of such irregular sets. Fractals have non-integer dimensionalities. Mandelbrot [1] coined the word, "Fractal" from the Latin word "fractus", (i.e., broken), to describe the objects that were too irregular to fit into a traditionally geometrical setting. Some examples: the middle third Cantor set, the von Koch curve, and the Sierpinski gasket [2]. These fractals are self-similar, i.e., on going from one length scale to the other they look the same. This property allows for applying the decimation technique.

To construct the Sierpinski gasket [3], we begin with an equilateral triangle. The midpoints of its edges are connected and create four equilateral triangles. The central triangle is removed and the same procedure is continued for each of the new triangles down to the microscopic lattice constant. It is better to think of this procedure as repeatedly replacing an equilateral triangle by three triangles of half the height. So, in the *m*th step of the construction the length scale is 2^{-m} and the area within the gasket is proportional to $2^{-m(2-D)}$ [3],

where $D = \ln 3/\ln 2$ is the fractal dimensionality of the gasket [4], which is of the solution $\sum_{1}^{3}\left(\frac{1}{2}\right)^{D} = 1$ (see Hausdorff dimension [2]). If no triangles were removed the area would be invariant scale and $D = 2$. We notice that the number of triangles in the gasket grows as 2^{mD} [3]. On going from one length scale to the other, the gasket appears the same, i.e., it is self-similar [5].

Because of the big number of spins (e.g., for ten steps $N_s = 88575$ spins) located on sites of the Sierpinski gasket, it is so difficult to get the partition function, $Z = \sum_{\{s\}} e^{-\beta H(s)}$ where the sum is extended over all possible states of the system. Therefore, the decimation technique (renormalization-group analysis) enables us to compute the partition function easily. A uniform system of spins on the Sierpinski gasket has been studied by Gefen *et al.* [4]. Cieplak *et al*. [6] have also applied the method of Gefen *et al*. on random spin systems in the absence of magnetic field. For any particular length scale the Hamiltonian for the gasket is equivalent to that for a triangle with renormalized exchange couplings [7]. Hikihara, *et al.* have calculated the ground-state two-spin correlation of spin-$\frac{1}{2}$ quantum Heisenberg chains with random exchange couplings using the real-space renormalization-group scheme [8]. Frontera *et al.* [9] have found that the distribution of random fields is continuous.

The aim of this paper is to investigate the influence of the external magnetic field on the distribution of the exchange couplings and the scaling stiffness energy for both the Gaussian and $\pm J$ models at zero and non-zero temperatures. Also the free energy per spin at zero temperature is studied versus both of the concentration of negative bonds (x) and the external magnetic field (B).

In the present work, we consider the disordered Ising spin glass (SG) and $\pm J$ model on a Sierpinski gasket placed in an external magnetic field. Their properties are numerically investigated by an exact decimation technique.

2. The model:

A triangular fragment of the Sierpinski gasket (Fig. (1)) spans two lattice spacings and consists of three corner and three midpoint spins. Consider a system of N_S Ising spins $S_i = \pm 1$ located on sites of the Sierpinski gasket placed into an external magnetic field B [9]. The Hamiltonian of our systems is given by:

$$H = -\sum_{\langle ij \rangle} J_{ij} S_i S_j - B \sum_{i=1}^{N_s} S_i \qquad (1)$$

where the nearest-neighbours couplings, J_{ij}'s are independent random numbers and B is the external uniform field. For SG, J_{ij}'s are generated from the Gaussian probability distribution with zero mean and unit dispersion. But for the $\pm J$ model, J_{ij}'s are generated from binary distribution.

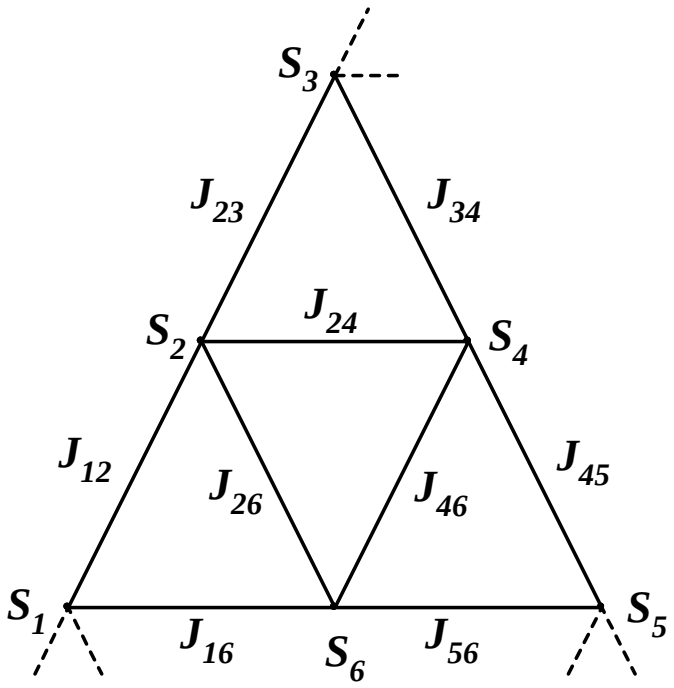

Fig. (1): Fragment of the Sierpinski gasket.

3. The decimation technique.

For fixed S_1, S_3 and S_5 there are eight possible energy states, $E_\lambda(\lambda = 1,2,...,8)$ of the unit, e.g., for $\lambda = 1$ we set $S_2 = S_4 = S_6 = 1$ and get:

$$\begin{aligned} E_1 = -\{&(J_{12} + J_{16})S_1 + (J_{23} + J_{34})S_3 + (J_{45} + J_{56})S_5 + J_{24} + J_{26} + J_{46} \\ &+ B(S_1 + S_3 + S_5 + 3)\} \end{aligned} \quad (2)$$

With each step of the decimation, the midpoint spins can be eliminated and the effective interactions J'_{ij}'s between the corner spins are found, so that:

$$\sum_{\lambda=1}^{8} e^{-\beta E_\lambda} = \exp\beta\left[C + J'_{13}S_1S_3 + J'_{35}S_3S_5 + J'_{15}S_1S_5 + B(S_1 + S_3 + S_5)\right] \quad (3)$$

At T=0, equation (3) is simplified as follows [6]:

$$\min_{\lambda}\{E_\lambda\} = -\left[C + J'_{13}S_1S_3 + J'_{35}S_3S_5 + J'_{15}S_1S + B(S_1 + S_3 + S_5)\right] \quad (4)$$

In each decimation step, nine exchange interactions for every unit, $(J_{12}, J_{23}, J_{34}, J_{45}, J_{56}, J_{16}, J_{24}, J_{46}, J_{26})$ are replaced by three effective exchange interactions, $(J'_{13}, J'_{35}, J'_{15})$, and a constant term C [7]. The constant term is of interest only when calculating the thermodynamic quantities [10]. The external magnetic field B breaks the system's global symmetry. So, the solution of equation (3) gives two groups of equations in the same four unknowns, $J'_{13}, J'_{35}, J'_{15}, and\ C$. We may combine these two groups for these unknowns by adding both sides of the equations and dividing by 2. This gives us the recursion relations

$$J'_{13} = \frac{1}{8\beta}\ln\left[\frac{A_1^+A_1^-A_2^+A_2^-}{A_3^+A_3^-A_4^+A_4^-}\right], \quad (5)$$

$$J'_{35} = \frac{1}{8\beta}\ln\left[\frac{A_1^+A_1^-A_4^+A_4^-}{A_2^+A_2^-A_3^+A_3^-}\right], \quad (6)$$

$$J'_{15} = \frac{1}{8\beta}\ln\left[\frac{A_1^+A_1^-A_3^+A_3^-}{A_2^+A_2^-A_4^+A_4^-}\right], \quad (7)$$

and

$$C = \frac{1}{8\beta} \ln\left[A_1^+ A_1^- A_2^+ A_2^- A_3^+ A_3^- A_4^+ A_4^-\right]. \tag{8}$$

where

$$A_q^{\pm} = 2\left\{e^{\beta\gamma_1} \cosh\beta\left(\alpha_{4q-3} \pm 3B\right) + \sum_{t=1}^{3} e^{\beta\gamma_{t+1}} \cosh\beta\left(\alpha_{4q+t-3} \pm B\right)\right\} \; ; \; q = 1,\ldots,4 \tag{9}$$

And $\alpha's$ and $\gamma's$ are defined as follows:

$$\begin{pmatrix} \alpha_1 \\ \alpha_2 \\ . \\ . \\ . \\ \alpha_{16} \end{pmatrix} = \begin{pmatrix} +1 & +1 & +1 & +1 & +1 & +1 \\ +1 & -1 & +1 & +1 & +1 & -1 \\ +1 & +1 & +1 & -1 & -1 & +1 \\ -1 & +1 & -1 & +1 & +1 & +1 \\ +1 & +1 & +1 & +1 & -1 & -1 \\ +1 & -1 & +1 & +1 & -1 & +1 \\ +1 & +1 & +1 & -1 & +1 & -1 \\ -1 & +1 & -1 & +1 & -1 & -1 \\ +1 & +1 & -1 & -1 & +1 & +1 \\ +1 & -1 & -1 & -1 & +1 & -1 \\ +1 & +1 & -1 & +1 & -1 & +1 \\ -1 & +1 & +1 & -1 & +1 & +1 \\ +1 & +1 & -1 & -1 & -1 & -1 \\ +1 & -1 & -1 & -1 & -1 & +1 \\ +1 & +1 & -1 & +1 & +1 & -1 \\ -1 & +1 & +1 & -1 & -1 & -1 \end{pmatrix} \begin{pmatrix} J_{12} \\ J_{16} \\ J_{23} \\ J_{34} \\ J_{45} \\ J_{56} \end{pmatrix} \tag{10}$$

and

$$\begin{pmatrix} \gamma_1 \\ \gamma_2 \\ \gamma_3 \\ \gamma_4 \end{pmatrix} = \begin{pmatrix} +1 & +1 & +1 \\ +1 & -1 & -1 \\ -1 & +1 & -1 \\ -1 & -1 & +1 \end{pmatrix} \begin{pmatrix} J_{24} \\ J_{26} \\ J_{46} \end{pmatrix} \tag{11}$$

The procedure is iterated recursively to yield renormalized values of the exchange couplings at each length scale. At each stage the triangles were combined into units and the decimation was performed by the same recursion relations (considering $J's$ as original exchange couplings for the next stage of decimation). The renormalized couplings were then combined into new units and so on [6]. The consecutive decimation stages are labelled by the index *m*.

For *m*=0 the description refers to the microscopic level. The corresponding length scale coincides with the lattice constant. For a general value of *m*, $N = 3^m$ of the original triangles are combined into one effective triangle. The corresponding length scale is then equal to $\ell = 2^m a$ [6]. The relation between the number of triangles combined in this way and the length scale of the description is given by $N = (l/a)^D$ where *D* is the fractal dimensionality of the gasket [6]. We consider a system with $N = 3^{10}$ triangles. Such a system consists of $N_S = \frac{3}{2}(N+1) = 88575$ spins and is characterized by 3^{11} exchange couplings.

4. Results and discussion

We calculated the flow of the probability distribution, scaling stiffness energy (ΔE_s), and the average of exchange couplings $\langle J \rangle$ and $\langle J^2 \rangle^{1/2}$ at each stage of decimation for several values of the external magnetic field *B*. These quantities were calculated for both SG and $\pm J$ models at zero and non-zero temperature.

4.1. SG Case:

Figure (2) shows several initial stages of the flow of the probability distribution for *x* = 0 the Gaussian case at $T = 0$ and *B* in the range $0 \le B \le 2$. The width of the probability distribution of the renormalized exchange couplings decreases algebraically when the applied external magnetic field is increased with the size of the system. At *B* = 1, all the couplings vanish after three iterations but at *B* = 2, they vanish after two. We found for *T* = 1 that the decrease in the width of the distribution is more than that for *T* = 0 and the probability distribution shrinks to the paramagnetic fixed probability distribution (FPD) $\delta(J)$ in case *T* = 1 more than in case *T* = 0. We notice that both of the external magnetic field and the temperature cause the width of the probability distribution of the renormalized exchange couplings to decrease when they increase. Fig. (3) shows the flow of the probability distribution in the Gaussian case at $T = 0$ and for $x = 0.5$ which is the spin glass case. The width of the probability distribution of the renormalized exchange couplings decreases with the size of the system when *B* is increased. At *B* = 2, all the couplings vanish after two iterations. The probability distribution shrinks more and more to the paramagnetic (FPD) $\delta(J)$, when *B* increases in the interval $0 \le B \le 2$. The width of the probability distribution is less for *T* = 1 than for *T* = 0.

For all *x*, the probability distribution at a given length scale can be represented schematically by [6]:

$$P(J) = h\delta(J) + (1-h)w(J) \tag{12}$$

Where $0 \le h \le 1$ and $w(J)$ represents the uniform portion.

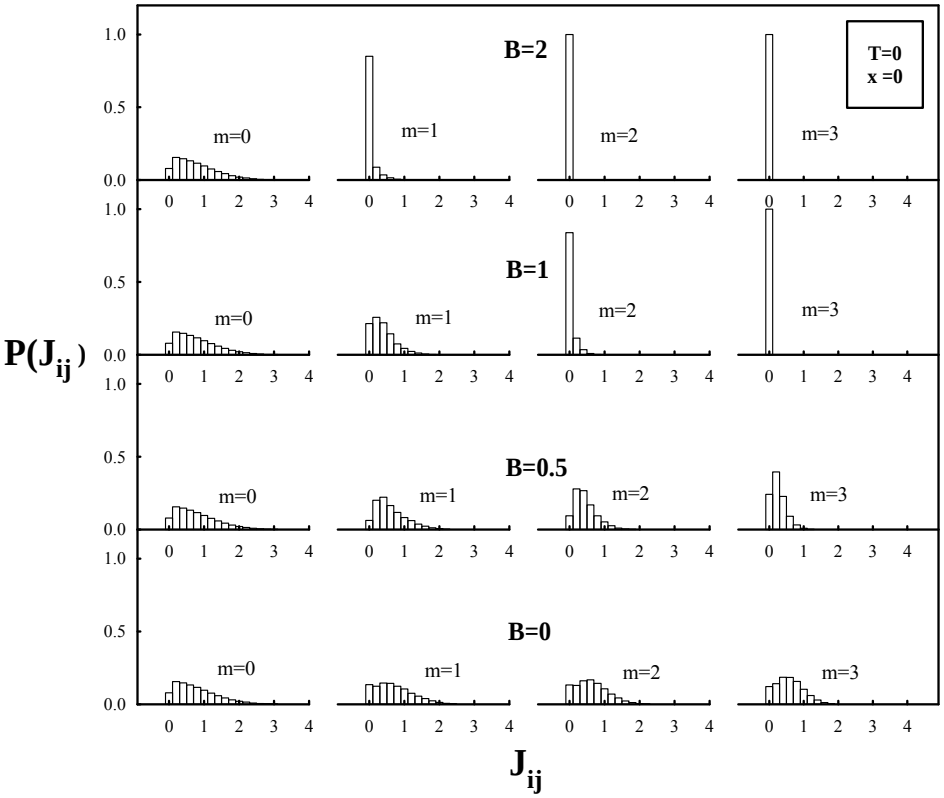

Fig. (2): Flow of the single-J probability distribution for $x = 0$ in the Gaussian model for several values of the external applied magnetic field (*B*) at T = 0.

Figure (4) demonstrates the scaling properties of stiffness energy (ΔE_s) at T = 0. At $B = 0$, ΔE_s scales with the size of the system algebraically and at B = 0.5, they scale algebraically until the fourth iteration and become constant for the remaining iterations. For $B = 1$ and 2, ΔE, stays constant after the second iteration for all values of *x*. We observe that with increasing the magnetic field, the scaling stiffness energy remains constant with the size of the system and for

all values of *x*. For $T = 1$, we found that ΔE_s delays to remain constant than for $T = 1$. Exponents *r* and *p* are defined as follows [6]:

$$< J > \approx N^{p} \tag{13}$$

$$< J^{2} >^{1/2} \approx N^{r}, \tag{14}$$

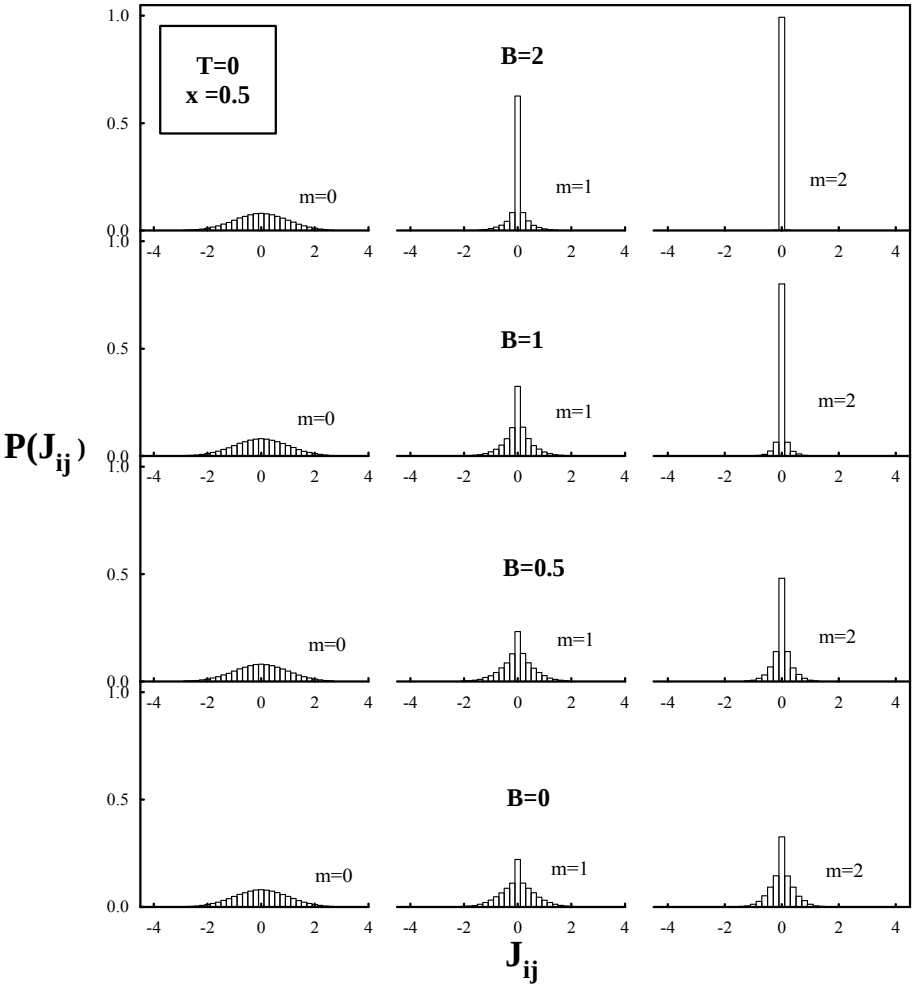

Fig. (3): Flow of the single-J probability distribution for $x = 0.5$ in the Gaussian model for several values of the external applied magnetic field (*B*) at T = 0.

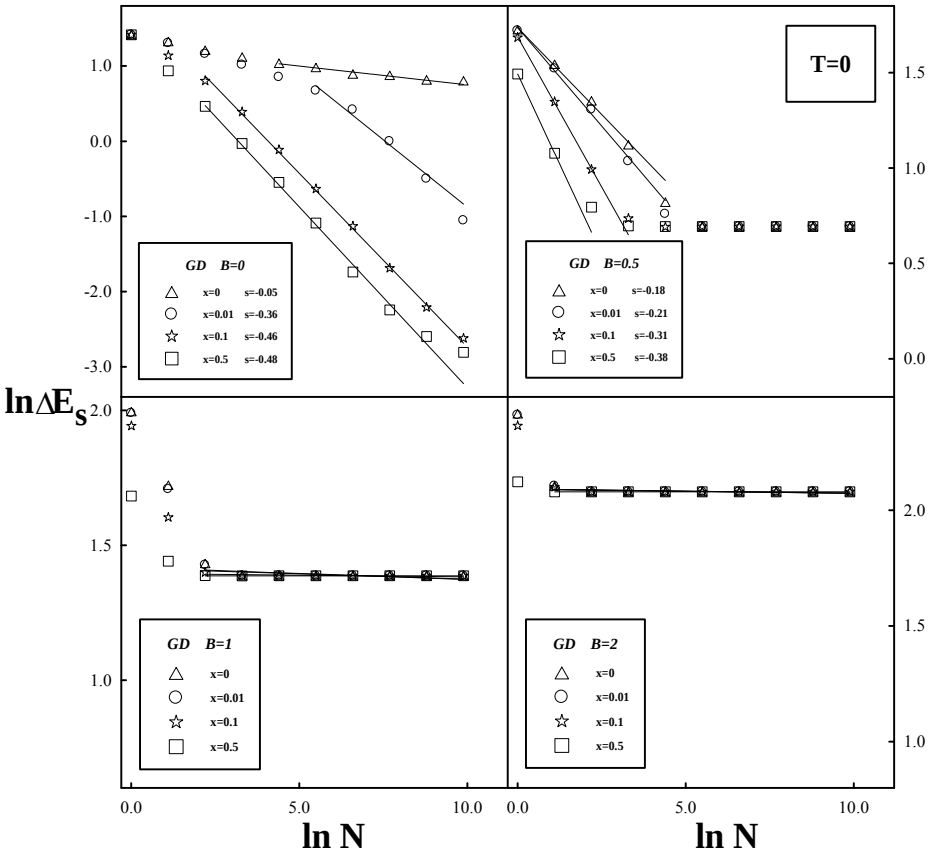

Fig. (4): $\ln \Delta E_s$ versus $\ln N$ in the Gaussian model for several values of concentration, *x* and for several values of external magnetic field (*B*) at T = 0. The corresponding slope is denoted by *s*.

A corresponding power law behavior holds [6] and $s = \max\{p, r\}$. Exponents *r* and s versus *x* are shown in Figure 5. It is seen that, as *B* increases the curves of both *r* and *s* are shifted vertically downward which means that they decrease with increase of *B*. These exponents are negative for all values of *x* and close to -0.04 for $x = 0$ and $B = 0$ and then they rapidly decrease. In the vicinity of $x = 0.13$ they level off at $s = r \approx -0.5$ and stay constant for all remaining values of *x*. The scaling properties of $\langle J \rangle$ and $\langle J^2 \rangle^{1/2}$ at $T = 0$ are shown in figure 6. It is seen that, for $x = 0$ and $B = 0$ the two quantities scale identically, i.e., $r = p = -0.05$ and the system is a disordered ferromagnet. As long as $x > 0$, a decay to zero for $\langle J \rangle$ is much faster than $\langle J^2 \rangle^{1/2}$ does and the

system is a spin glass. It is clear that at $T=0$, $\langle J^2\rangle^{1/2}$ decays in an algebraic fashion, while power law fits to $\langle J\rangle$. Across $B\geq 1$, $\langle J\rangle$ and $\langle J^2\rangle^{1/2}$ approach zero very fast. At $T=1$, the values of Both $\langle J\rangle$ and $\langle J^2\rangle^{1/2}$ are less dependence on *x* than $T=0$ case.

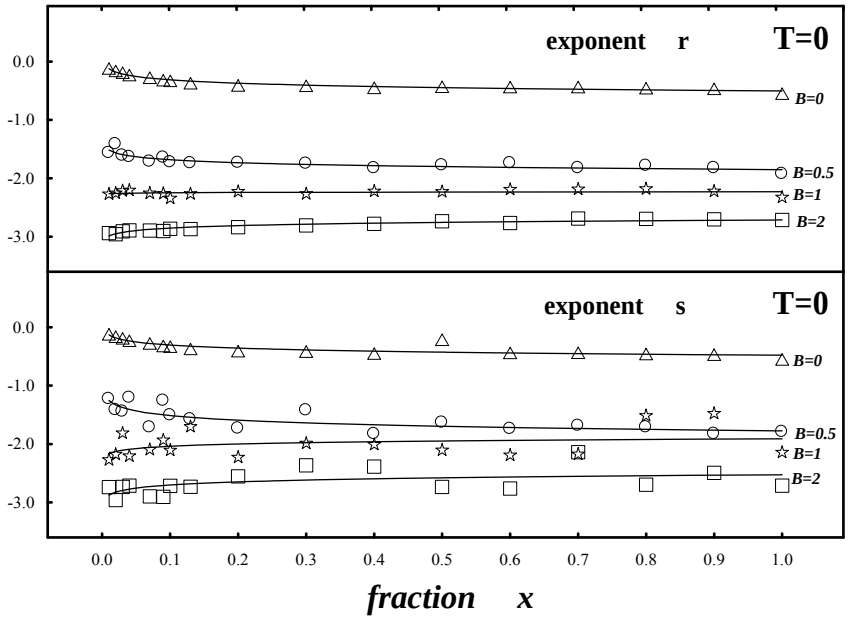

Fig. (5): Exponent *r*, defined in equation (14) and exponent *s*, for ΔE_s as a function of concentration of negative bonds *x* in the Gaussian model for several values of *B*.

Actually, much better description of $\langle J\rangle$ is given by the following law [6].

$$\langle J\rangle \approx \frac{e^{-(N/\eta)^{\alpha}}}{N^{0.04}} \qquad (15)$$

Both the evidence for this law and the influence of *B* and the plot of $\ln\left(-\ln\left(\langle J\rangle N^{0.04}\right)\right)$ as a function of $\ln N$ are presented in Fig. (7), at *T* = 0. The slope α depends on *x*, in a way, weakly and is greater at *T* = 1 than at *T* = 0. The intersection with the vertical axis at *N* = 1 yields $-\alpha\ln\eta$ which allows for determination of η. By increasing B the system becomes more ordering. We note that the slope converges as the external magnetic field increases. Fig. (8) shows the dependence of η on *x*. We observe that: η exponentially decays as *x*

increases for $B = 0$ and 0.5. But for $B = 1$ and 2, it decays algebraically. We see that when $x \to 0$ then η diverges as [6]:

$$\eta \approx x^{-\mu} \tag{16}$$

The quantity η will be called as the ferromagnetic coherence length since it characterizes the spatial extent of the incipient ferromagnetic order.

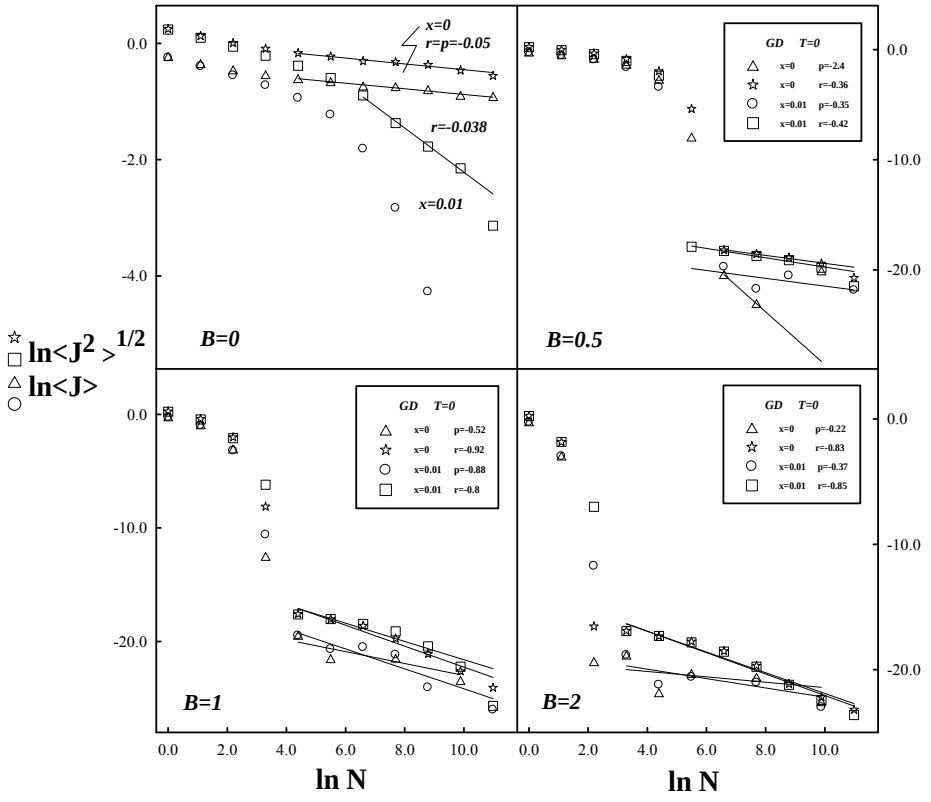

Fig. (6): $< J >$ and $< J^2 >^{1/2}$ on the log-log plane for the Gaussian model at $x = 0$ and $x = 0.01$ for several values of B at T = 0.

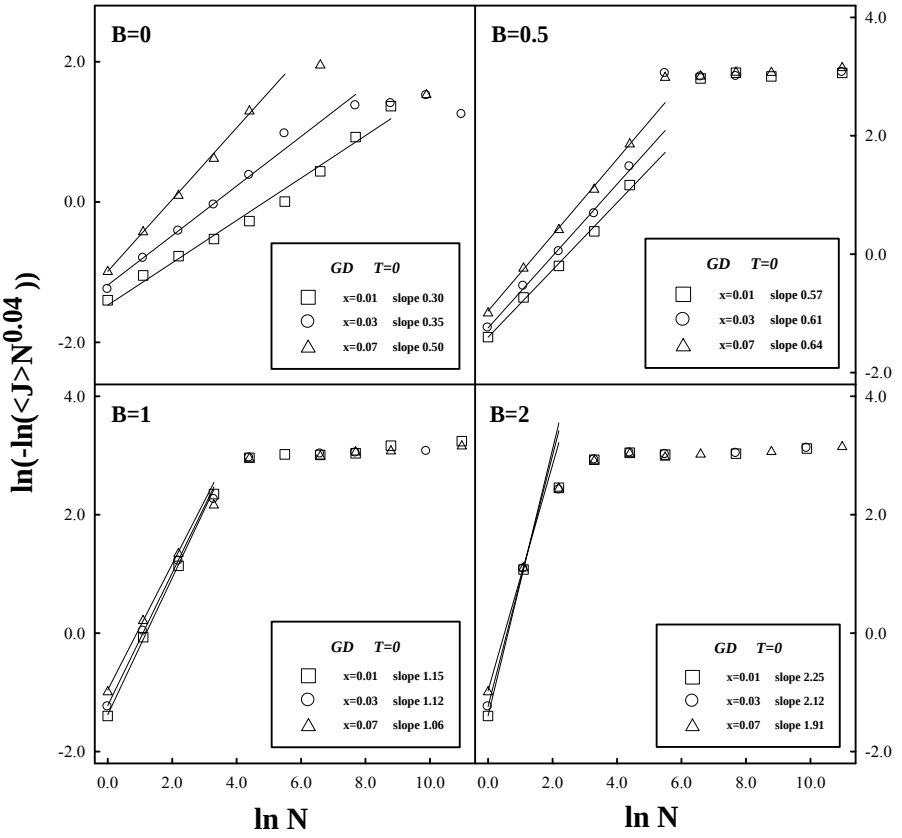

Fig. (7): Evidence for the validity of equation (15) for the Gaussian model at $x = 0.01, 0.03 \text{ and } 0.07$ and for several values B at T = 0

4.2. ± J Case:

The flow in the $\pm J$ system at $x = 0.03$ and at $T = 0$ for several values of an external magnetic field is shown in Fig. (9). At $T = 0$, only discrete values of J are allowed. At $B = 0$, the bins corresponding to $J = \pm 1$ become depleted and give rise to the $J = 0,1$ effective couplings. At B = 0.5, the distribution at the value of $J = 1$ depletes and many values of the effective couplings rise between 0 and 1. At B = 1, also discrete values rise but of value less than 1 and all the couplings vanish at the third step of decimation. Finally, when B = 2, all the couplings are equal to zero with first iteration. When T = 1 the values of $J's$ deplete and dense values appear greater than those at T = 0.

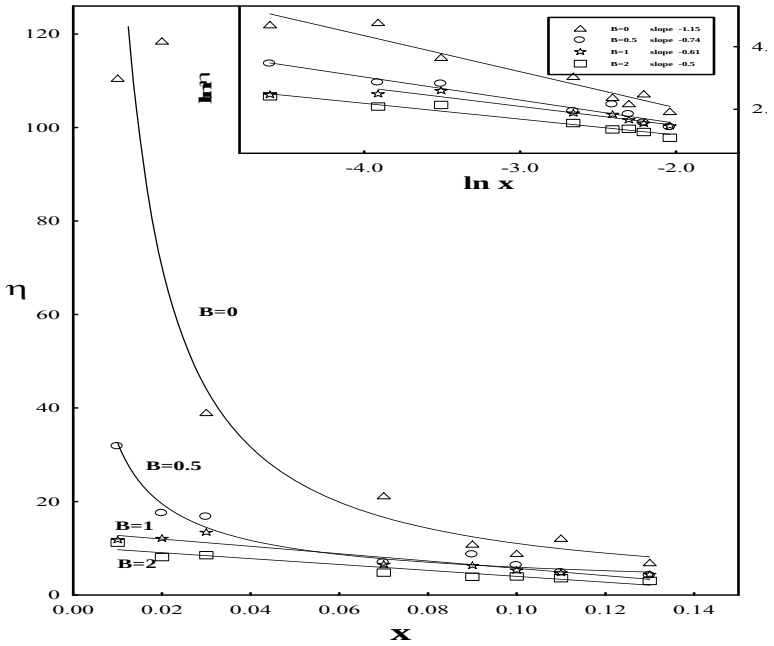

Fig. (8): Dependence of the ferromagnetic coherence length η on x in the Gaussian model for several values B. The insert shows the log-log plot to prove the validity of Eqn. (16).

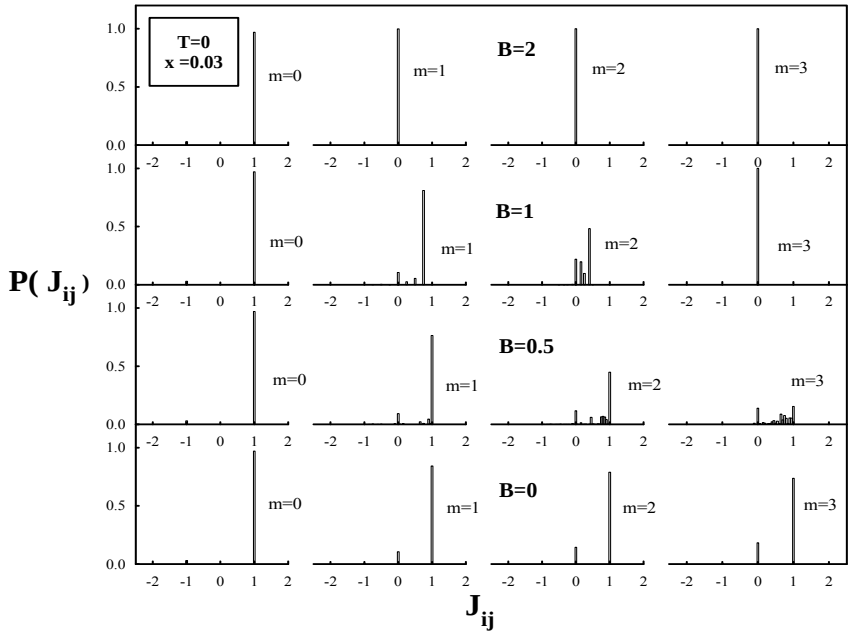

Fig. (9): Flow of the probability distribution for $x = 0.03$ for several values of B in the $\pm J$ model at T = 0.

Figure (10) demonstrates the scaling properties of ΔE_s at $T = 0$. It is seen that for all $x > 0$ at $T = 0$, ΔE_S depends on N exponentially and the system is then paramagnetic. The slope decreases with increasing of B in the two concentrations, $x = 0.1$ and 0.5. For non-zero temperature ($T = 1$) and when B is increased ΔE_S is less in its dependence on x. Fig. (11) shows the behavior of $\langle J \rangle$ and $\langle J^2 \rangle^{1/2}$. We note that $\langle J \rangle$ decays faster than $\langle J^2 \rangle^{1/2}$ which indicates that the system is dominated by frustration. When the external field increases the frustration decreases. Both of $\langle J \rangle$ and $\langle J^2 \rangle^{1/2}$ decrease with increasing B. The slope at T = 1 is greater than at T = 0.

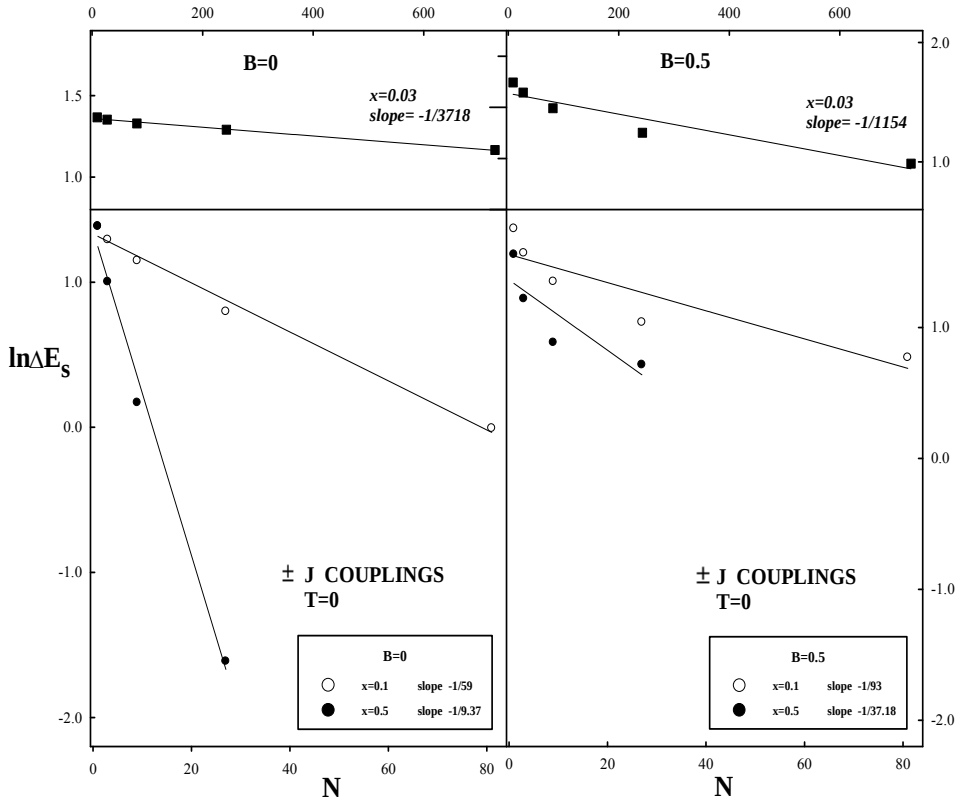

Fig. (10): Plot of $\ln \Delta E_s$ versus N for several values of B in the $\pm J$ model and for several concentrations of the negative bonds at $T = 0$.

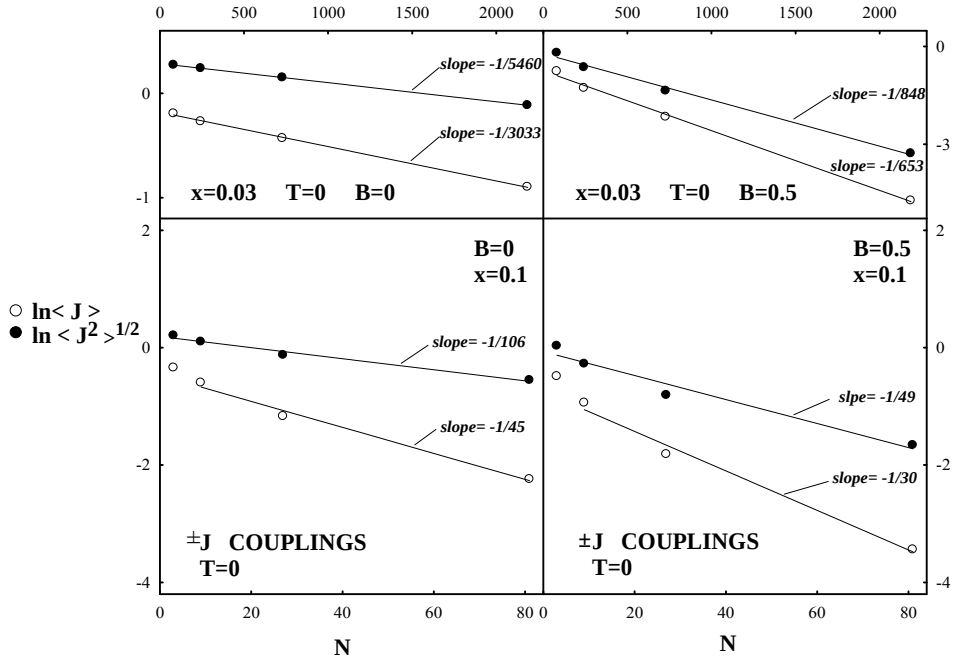

Fig. (11): Plots of $\ln < J >$ and $\ln < J^2 >^{1/2}$ versus N for several values of B in the $\pm J$ model at $T = 0$.

5. The free energy

Numerically the free energy per pin is exactly calculated for N_s = 88575 using [11,12]:

$$F = -\frac{K_B T}{N_s} \ln Z\{J_{ij}, B\} \qquad (17)$$

Figure (12) shows that the free energy per spin increases with the concentration (x). It is clear that the free energy per spin grows in an algebraic fashion. At several values of the external magnetic field in the range $0 \le B \le 3$ the curves of free energy per spin have a vertical shift downward as B increases in this range. Fig. (13) shows that the free energy per spin decreases with the external magnetic field. We notice the vertical shift when the concentration (x) increases.

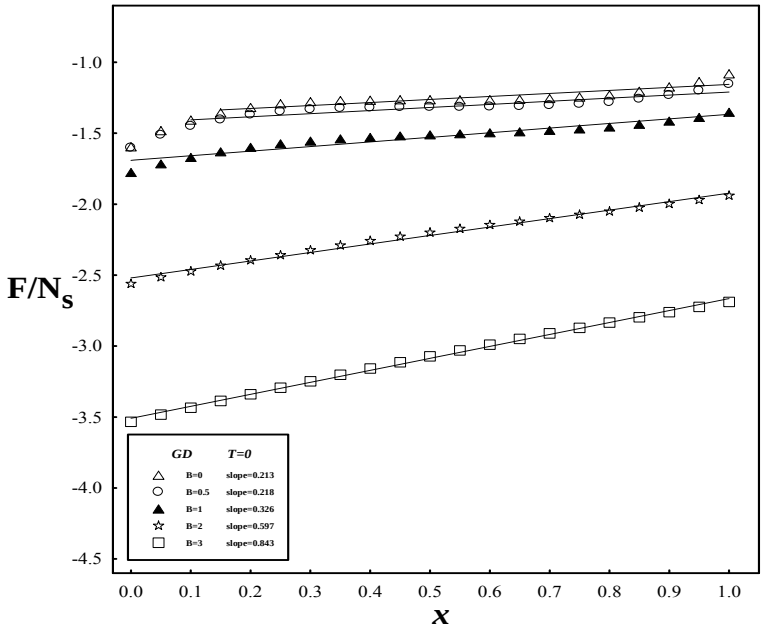

Fig. (12): Free energy per spin F versus concentration of negative bonds x at $T = 0$ and for several values of B in the Gaussian model.

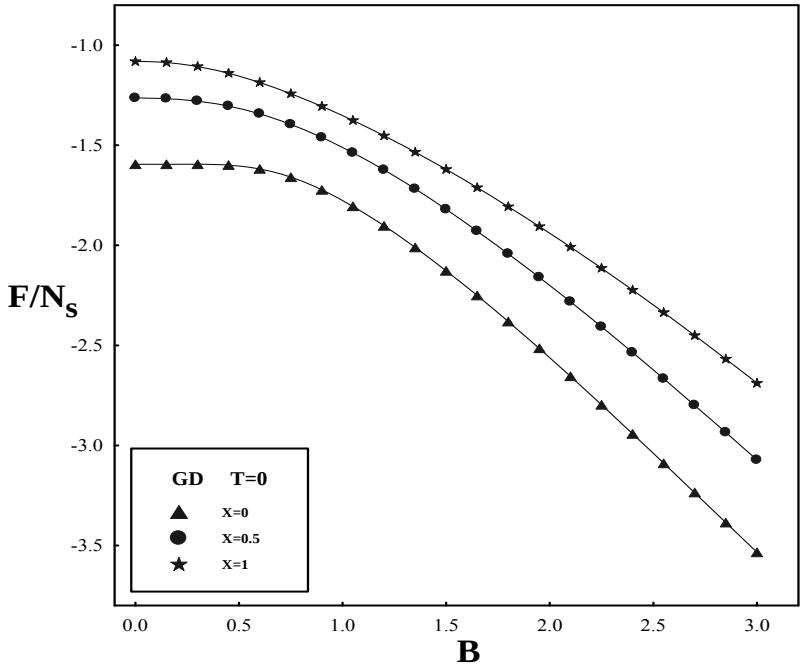

Fig. (13): Free energy per spin F versus external magnetic field B at $T = 0$ for several values of x in the Gaussian model.

6. Conclusion:

Our problem was treated numerically and formulated by a FORTRAN program and the obtained data was plotted. In Gaussian case (SG), we found that the width of the flow of the probability distribution for x = 0.1 and 0.5, decays with increasing the magnetic field until all the couplings vanish. We notice that the greater the temperature the less the width of the distribution of the exchange couplings. For $\pm J$ model, the magnetic field makes the values of $\pm J$ deplete and discrete values give rise between $J = 0$ and $J = 1$. The scaling stiffness energy decays algebraically with the size of the system and when the magnetic field increases it becomes constant for all values of *x*. We found that when *B* increases both $\langle J \rangle$ and $\langle J^2 \rangle^{1/2}$ approach to zero very fast. Exponents *r* and *s* decrease with increasing *B*. The flow in the $\pm J$ case at $x = 0.03$ and at T = 0 and 1, ΔE_S depends on *N* exponentially and when *B* is increased its slope decreases to become near to zero at *B* = 2 (i.e., ΔE_s is constant). We notice that $\langle J \rangle$ and $\langle J^2 \rangle^{1/2}$ decrease with increasing *B*. The free energy increases with increasing *x* but it decreases with increasing *B*.

References

1. M. Batty**:** "*Fractals-geometry between dimensions*", New Scientist 4 April (1985).

2. K. J. Falconer**:** "*Fractal Geometry Mathematical Foundations and Applications*" Bristol**,** April 1989.

3. M. Cieplak and J.R. Banavar**:** *Springer Series in Solid State Sciences*, **54**, 115 (1984).

4. Y. Gefen**,** B. B. Mandelbrot and A. Aharony**:** *Phys. Rev. Lett*. **45**, 855 (1980).

5. Y. Gefen**,** A. Aharony**,** B. B. Mandelbrot and S. Kirkpatrick**:** *Phys. Rev. Lett*. **47**, 1771 (1981).

6. M. Ciepak**,** P. Cieplak and M. A. Kotur**:** J. *Phys. C* **19**, 4063 (1986).

7. J. R. Banavar and M. Cieplak**:** *Phys. Rev. B* **28**, 3813 (1983).

8. T. Hikihara, A. Furusaki and M. Sigrist **:** *Phys. Rev*. B **60** 12116 (1999).

9. C. Frontera**,** J. Goicoechea**,** J. Ortin and E. Vives **:** *J. Comp. Phys*. **160**, 117 (2000).

10. J. H. Luscombe and R. C. Desai**:** *Phys. Lett.* **108A**, 39 (1985).

11. I. Morgenstern and K. Binder **:** *Phys. Rev. Lett*. **43,** 1615 (1979).

12. M. Cieplak and M. Z. Cieplak **:** *Phys. Rev. B* **26,** 2482 (1982).